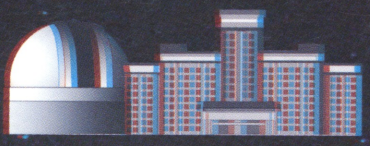

200th Anniversary of Astronomy in Kharkiv

International Conference

SOLAR SYSTEM BODIES: FROM OPTICS TO GEOLOGY

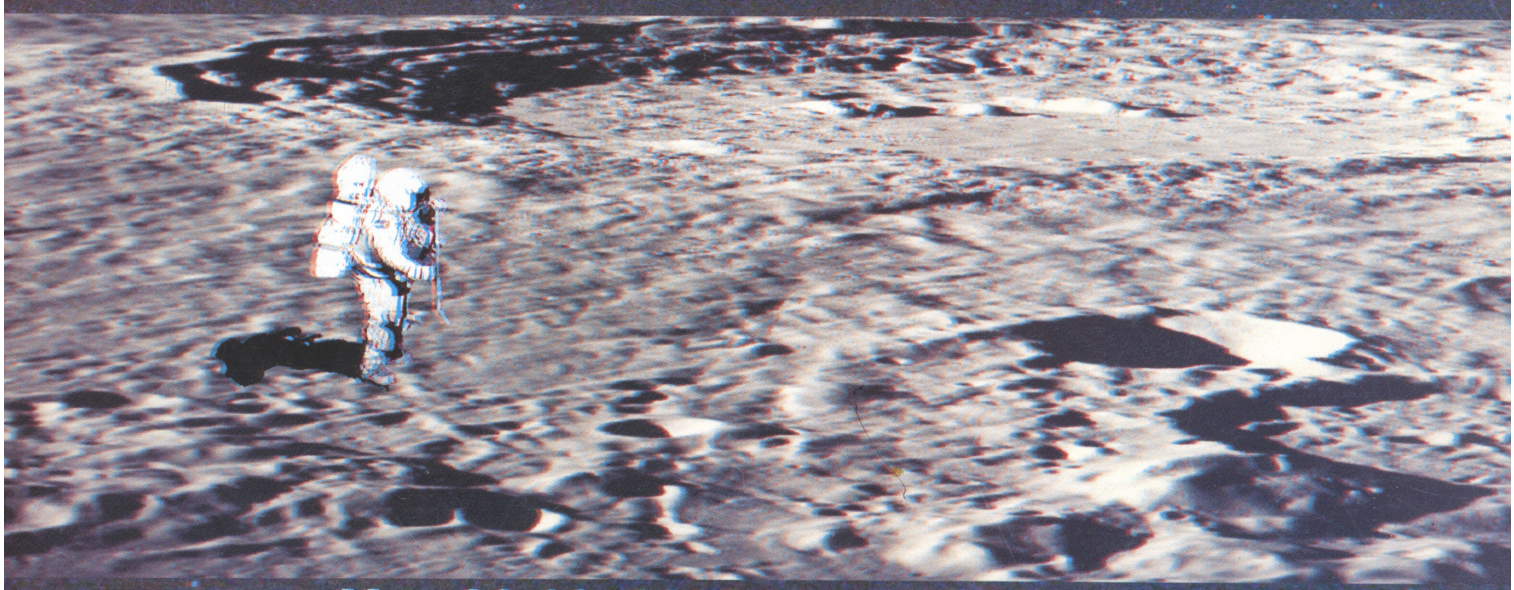

May 26-29, 2008, Kharkiv, Ukraine

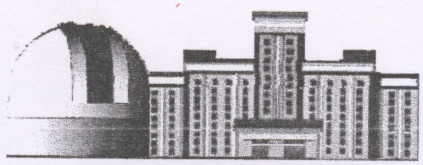

200th Anniversary of Astronomy in Kharkiv

International Conference

THE SOLAR SYSTEM BODIES: FROM OPTICS TO GEOLOGY

May 26–29, 2008, Kharkiv, Ukraine

ABSTRACT BOOK

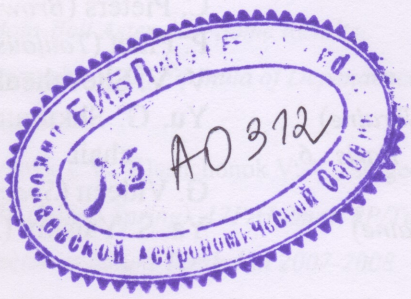

ФОНД ОЛЕКСАНДРА ФЕЛЬДМАНА

esa

USE OF THE COMBINED CCD OBSERVATION METHOD FOR FAST NEAR EARTH OBJECT OBSERVATIONS IN RI NAO.

O. Shulga, Y. Kozyryev, Y. Sibiryakova. Research Institute "Nikolaev Astronomical Observatory" (RI NAO), Ukraine, tttt_nao@mail.ru.

There is a difficulty of observation of the fast NEO objects with speed V > 10"/sec. That type of objects can't be observed in prolonged exposure with classical way which is used for observing stars. So limiting magnitude of telescope can not be reached. In order to increase magnitude of observing objects the selection of tracking mode is necessary. It is possible to have the following tracking modes:

- Digital - stacking of shifted images obtained in short exposure time;
- Mechanical - moving telescope around its two axes precisely;
- Electronic - tracing of electronic charge through the CCD matrix.

The electronic tracking technique was designed in RI NAO. Observation is carrying out while object is passing through the field of view of unmovable telescope. So limited exposure time is depends from object speed and field of view size. This method can be used for observation of objects with any visible speed: from stars to low Earth orbit satellites.

The electronic tracing technique, designed in RI NAO, is based on Drift-Scan Imaging or Time Delayed Integration (TDI). The Drift-Scan Imaging technique is usually used to image long continuous strips of the sky. To make a scan it is necessary to read the lines of the CCD in perfect synchronization with the movement of the stars at the focal plane. It is also important to perfectly align the lines with east-west direction. In RI NAO this technique has been used on Meridian Circle telescope since 1995. The field of application of the Drift-Scan Imaging technique can be extended considerably with possibility of rotation of the CCD camera to the certain angel. In that case it can be used for observation of any object which is uniformly moving through the field of view. For that purpose special rotation system (image 1) was designed in RI NAO. The rotation system is a device in which a stepping motor and an angle encoder were equipped and which makes the rotation of CCD camera around telescope optical axis.

The electronic tracing technique was tested on very small telescope so only relative advantage can be showed. The test observation of asteroid 2007 TU24 was realized with use this method. On 2008-01-30 the asteroid speed was -9.3"/min on right accession, -28.9"/min on declination, magnitude 12.1. The asteroid was observed on an unmovable telescope with the classical drift-scan imaging technique and with the rotation system (image 2). Exposure time - 240 sec, so while the exposure time the asteroid have passed 120" or 55 pixels.

Images obtained with object tracking mode (mechanical or electronic) contains round image of object but stretched images of stars which are difficult for data reduction. To avoid this problem the special additional frames with different mode are made before and after object frame.

Image 1. Rotation system with CCD camera

Image 2. Images from different drift-scan observations. Left: Classical drift-scan imaging, right: Drift-scan imaging with rotation system

Telescope is unmovable so it not a problem to connect the object coordinates and the reference stars coordinates obtained on different frames in different time. The easiest way to obtain reference stars frame on stare telescope is to use very short exposure time. While observation of the fast NEO objects on an unmovable telescope it is possible to use driftscan imaging with variable small exposure time to obtain reference stars frame.

The electronic tracking technique can provide results which are comparable to observations on precise tracking telescope for wide object types from fast NEO objects to fast low Earth orbit satellites. The most telescopes in Ukraine and Russia which are used for asteroids observations are old and can't track any objects except stars. The most easier and inexpensive way of modernization for tracking capability is to install the rotating system and CCD camera which support driftscan mode. RI NAO collaborating with Shanghai Astronomical Observatory carries out the common project in use of the electronic tracking technique.

THEORETICAL MODELING OF OPTICAL MATURATION OF LUNAR AND MERCURIAN REGOLITH. L. V. Starukhina, Yu. G. Shkuratov. Astronomical Institute of Kharkov University, Kharkov, 61022. Ukraine, starukhina@astron.kharkov.ua

Introduction: Spectral measurements provide information about chemical composition of the surfaces of celestial bodies. For atmosphereless bodies, spectral information is masked by space weathering that occur due to meteoritic bombardment or solar wind irradiation and results in maturation of the surface material (regolith). This emphasizes the importance of theoretical modeling for interpretation of the spectra.

Studies lunar samples showed that space weathering results in formation of grains of reduced metals, mainly iron, in silicate particles [1]. Lunar soils of low maturity contain mostly nanograins of Fe^0 ($npFe^0$), their average diameter being 50-60 Å, located in ~1000-2000 Å-thick amorphous outer zones of regolith particles; in mature soils, especially in impact glass, $npFe^0$, as well as Fe^0-grains of sizes up to a few microns, are distributed all over the particle volume [2].

Spectral effects of these structural changes are (1) darkening, (2) reddening and (3) decrease of the depths of absorption bands of ferrous ions (Fe^{2+}) near 0.95 and 1.85 μm [3,4]. Mercury that is supposed to have silicate composition show no absorption in spectral range from 0.4 μm to 1 μm. This suggested low iron content estimated by different authors from 5.5 wt.% FeO [5] to as low as 1.2 wt.% [6]. Another possible interpretation of the Mercurian spectrum is an extreme maturity of the surface due to processes called overmaturation [7].

To answer the question if Mercurian spectrum can impose any constraints upon its surface composition, theoretical simulation of the effects of space weathering on spectra of silicates, as well as theoretical modeling of the mechanisms of maturation are required. Here we consider both aspects of the problem.

Calculation of spectral effects of space weathering: The model of spectral reflectance of multicomponent regolith-like surfaces [8,9] enables us to calculate the spectrum of mature soil starting from that of immature one (or vise versa). At first, we calculate the spectrum of the imaginary part κ of the refractive index of the soil material using its reflectance spectrum. Next, the κ spectrum is modified by adding the contribution of $npFe^0$ to κ that can be obtained from Mie theory:

$$\kappa_{Fe} = (3/2)(\Delta c)n\cdot\mathrm{Im}[(\varepsilon-1)/(\varepsilon-2)], \quad (1)$$

where Δc is the difference in average volume concentration of $npFe^0$, n is the real part of silicate refractive index, and ε is the ratio of the complex dielectric constant of Fe^0 to that of silicate. Then reflectance spectrum is calculated for the modified κ spectrum and a new value of particle size.

The theoretical model was tested on spectra of particle size separates of lunar soils [8,9]. An example of theoretical simulation of the effects of space weathering on spectra of a lunar soil is given in Fig.1. The spectrum of bulk soil, which is controlled by particles of sizes <20μm [10], is obtained from the spectrum of less mature 20-40 μm size fraction. As shown in Fig.1, decrease of particle size brightens the spectrum, but only addition of $npFe^0$ in the abundance observed in lunar samples increases the slope enough to reproduce spectrum of more mature soil.

In Fig. 2 simulation of Mercury spectrum starting from that of a lunar sample is presented. The example is chosen among those measured by Lunar Soil Characterization Consortium [10] to show that even high FeO content (15 wt.%) of mare soil can be consistent with Mercury spectrum provided that particle size is small and $\Delta c \sim 10^{-3}$ that corresponds to ~0.1 wt.% of FeO. This is about maximal concentration of $npFe^0$ consistent with rather high albedo of Mercury at reasonable comminution of the surface particles.

However, the spectrum of the lunar sample taken for this example (line 1 in Fig.2) is rather exceptional for lunar soil spectra because of the lack of typical camber at about 0.75 μm (compare Fig.1).

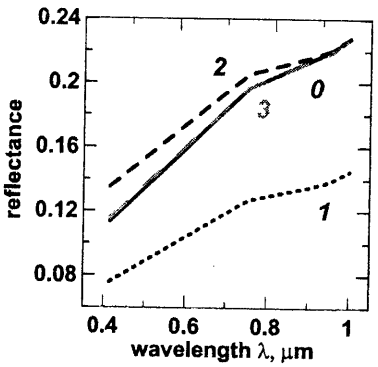

Fig.1. Simulation of bulk spectrum of lunar sample 61141 (*0*) starting from spectrum (*1*) of 20-40 μm size fraction: decrease of the average particle size *l* to 19 μm (*2*) and decrease of *l* to 16 μm combined with adding of $1.5\cdot10^{-2}$ vol.% of nano-Fe^0 grains (*3*).

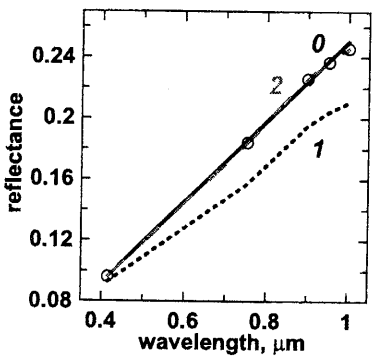

Fig.2. Mercury spectrum (*0*) and its simulation (*2*) starting from spectrum (*1*) of 5-10 μm size fraction of lunar sample 71061 with 15 wt.% of FeO; 1 is reduced by a factor of 1.7, and 0.1 vol.% of $npFe^0$ is added.

Simulation have shown that this upward bent cannot be removed by addition of $npFe^0$. The bent practically disappears at high Δc, but appears again when particle size is decreased enough to compensate darkening yielded by $npFe^0$. The lack of the upward bent for the lunar soil spectrum shown in Fig.2 can be due to the fact that significant part (25%) of FeO is contained in opaque ilmenite mineral, most of the rest iron being in glass component, probably, in large ($\geq \lambda$) Fe^0-grains.

Large grains of absorbing materials are opaque; so grain growth changes light absorption to scattering and provides brightening of a soil. Consider such a possibility for Mercurian surface.

Maturation mechanisms for silicate soils and extralunar extrapolations: In 70-80th there were discussions as to which of the space weathering agents – protons of solar wind or impact vapor produced in meteoritic bombardment – cause reduction of Fe in maturation. Thermodynamic data for Fe-FeO equilibrium [11] indicate that high temperature and low oxygen pressure are sufficient for reduction of Fe (Fig. 3), i.e., no additional reducing agents are required. This was confirmed in laser heating experiments with silicates (e.g.,[12]). Thus, the lack of protons on Mercurian surface protected from solar wind by magnetic field cannot prevent soil maturation.

As shown in [13], even impact melting is sufficient for $npFe^0$ formation on airless bodies, since $npFe^0$ formation rate in melt is faster than cooling rate. Impacts of submicron scale may be responsible for $npFe^0$ in the rims of regolith particles, whereas micron-scale Fe^0 grains can grow in particle volumes due to submillimeter impactors.

Meteoritic flux and impact velocity on Mercury are greater than for the Moon [5], so much more impact melt and vapor can be expected [5] and hence, much more impact glass and reduced iron on Mercurian surface as compared to the Moon.

Overmaturation of regolith as a mechanism of removal iron spectral features. High temperature on Mercurian surface enhances diffusion of atoms, which favors so called ripening in space-weathered silicate particles. The largest grains among the numerous $npFe^0$ grow at the expense of the smaller ones, their number decreasing by many orders of magnitude, their size increasing up to a few microns. The kinetics of Fe^0 grain growth in typical Fe-bearing silicate was calculated in [7] on the base of ripening theory [14] and diffusion data [15] (Fig.4).

Conclusions: (1) Impact melting can provide the observed characteristics of mature soils without any additional maturation mechanisms. Consequently, the mechanism may cause regolith maturation on bodies shielded from solar wind irradiation, such as Mercury, and on asteroids where collision velocities are sufficient for impact melting only.

(2) Intensive meteoritic bombardment on Mercury can result in reduction of almost all Fe^{2+}, formation of impact glass and $npFe_0$; high surface temperature allows growth of most of the Fe^0 grains to sizes when light absorption changes to light scattering, which brightens the surface.

(3) Optical spectrum of Mercury does not enable us to put any constrains on the abundance of iron on the Mercurian surface. Reduction and growth can mask iron in surface material up to concentrations typical of lunar mare soils. Limits for iron content on the surface of Mercury can be established on the base of geological models.

References: [1] Vinogradov A. P. et al. (1972) *Proc. Lunar Sci. Conf. 3d*, 1421-1427. [2] Morris R. (1977) *Proc. LPSC 8th*, 3719-3747. [3] Housley R. et al. (1973) *Proc. Lunar Sci. Conf. 4th*, 2737-2749. [4] Pieters C. M. et al. *J. Geoph. Res. 98*. 20817-20824. [5] Cintala M. J. (1992) *J. Geooph. Res. 97*, 947-973. [6] Warell J., and Blewett D. T. (2004) *Icarus 168*, 257-276. [7] Starukhina L. V. and Shkuratov Yu. G.. (2003) *LPSC XXXIV*, Abstr.#1224. [8] Starukhina L. V. et al. (1994) *LPSC XXV*, 1333-1334. [9] Starukhina L. V. and Shkuratov Yu. G.. (1996) *Solar System Res., 30*, 258-264. [10] Taylor L. A. et al. (2001) *J. Geoph. Res.*, **106**, 27985-28000. [11] O'Nell H. St. C. (1988) *Amer. Mineral. 73*, 470-486. [12] Moroz L. V. (1996) *Icarus 122*, 366-382. [13] Starukhina L. V. (2006) *LPSC XXXVII*, Abstr. # 1147. [14] Lifshitz I. M., Slyozov V. V. (1961). *J. Phys. Chem. Solids 19*, 35-50. [15] Buening D. K., and Buseck P. R. (1973) *J. Geoph. Res. 78*, 6852-6862.

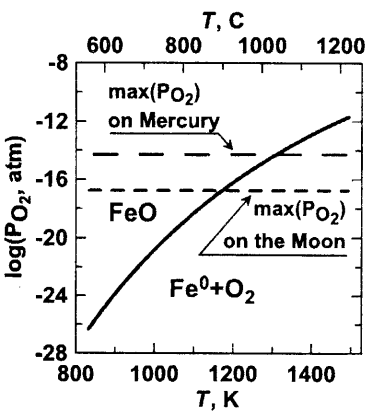

Fig.3. Thermodynamic conditions of iron reduction.

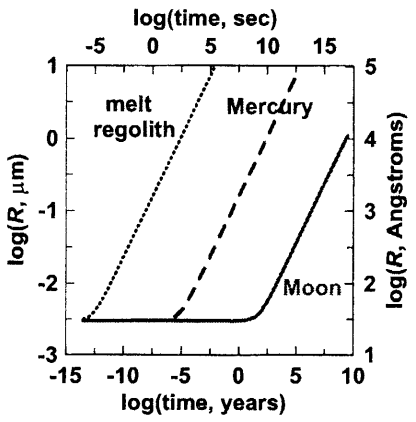

Fig.4. Rate of grain growth for reduced iron in olivine at day temperatures of the Moon and Mercury.

OBSERVATIONS OF BRIGHTNESS BEHAVIOR OF ASTEROIDS AT LOW PHASE ANGLES.

I. A. Tereschenko[1], V. G. Shevchenko[1], V. G. Chiorny[1], Yu. N. Krugly[1], I. N. Belskaya[1], N. M. Gaftonyuk[2], F. P. Velichko[1]. [1]Institute of Astronomy of Kharkiv Karazin National University, Sumska Str. 35, Kharkiv 61022, Ukraine, shevchenko@astron.kharkov.ua.[2]Crimean Astrophysical Observatory, Crimea, Simeiz 98680, Ukraine

Introduction: Continuing of the program for study of brightness behavior at low phase angle we have carried out new CCD-observations of some different type asteroids, devoting more attention for asteroids whose albedos lie in the range of 0.036-0.060 (for eleven objects). As it was pointed out in [1], lowalbedo asteroids show the smallest amplitude of the opposition effect (OE) and the largest dispersion of amplitude OE as compared to other asteroid types. The observations including low phase angles (<1 deg) and linear part of phase dependence have been performed for sixteen asteroids, namely: 76 Freia , 122 Gerda, 176 Iduna, 190 Ismene, 214 Aschera, 218 Bianca, 250 Bettina, 303 Josephina, 309 Fraternitas, 313 Chaldaea, 444 Gyptis, 615 Roswitha, 635 Vundtia, 717 Wisibada, 954 Li and 1279 Uganda. For some asteroids the observations carried out in four BVRI standard bands. Some physical characteristics namely: taxonomic type, albedo, diameter, rotation period, lightcurve amplitude, minimal phase angle, amplitude of OE, determined values of the H and G parameters and color indices B-V, V-R, and R-I of the observed asteroids are presented in the Table.

Results and discussion: The observations of the selected asteroids were carried out in 1999-2007 at the Institute of Astronomy of the Kharkiv Karazin National University (70 cm reflector) jointly with the Simeiz Department of the Crimean Astrophysical Observatory (1 m reflector), using ST-6, IMG-1024 and IMG 47-10 CCD-cameras. The accuracy of magnitudes for the individual nights is not worse than 0.02 mag. The accuracy of the color indices for the individual night is equal to 0.02 – 0.03 mag. As a result of series of photometric observations we have obtained the magnitude- phase relations for ten asteroids and the observations of other objects are in preparation. The magnitudes we adduced to main maximum of lightcurve to decrease an influence of lightcurve amplitude increasing with phase angle.

We have determined new and improved available values of the rotation periods of the observed asteroids and obtained the lightcurve amplitudes for some of them. The new more accurately determined values of the absolute magnitudes can be used for more precise estimation of albedos and/or diameters of these asteroids. The figures show phase dependence of brightness for some asteroids in four BVRI bands: 190 Ismene, 214 Aschera, 303 Josephina, and 615 Roswitha.

Magnitude-phase relation of asteroid 190 Ismene shows the very small amplitude of OE among lowalbedo asteroids. Values of amplitude of OE in four BVRI bands are close between themselves. It is possible that only the shadowhiding mechanism forms opposition brightness for this asteroid. Our observations allowed also to icrease the set of magnitude-phase relations for lowalbedo asteroids. We calculated a mean value of amplitude OE in V band for six lowalbedo asteroids from our set (excluding 190 Ismene and 444 Gyptis) that is equal to 0.16 mag and compared with that obtained by [1] for C-type asteroids. These amplitudes of OE are equally and we can suppose that the mean amplitude of OE maybe close to 0.16 mag for dark asteroids. The differences in the OE amplitudes of some asteroids from the mean value can be due to their individual surface features.

The magnitude- phase relations of E-type asteroid 214 Aschera shows a linear behavior of brightness up to phase angle about 1 deg and the sharp nonlinear increasing begins only at phase angles less than 1 deg. That is different from other E-asteroids 44 Nysa and 64 Angelina for which the spike- effect begins at phase angles less than 2 deg [2]. Amplitude of OE is equal to 0.10 mag that is also different from amplitudes of OE of 44 Nysa (0.14 mag) and 64 Angelina (0.16 mag). The amplitudes of OE of this asteroid in other spectral bands are close to a value in V band with accuracy to observation errors. We did not search any anomalies in behavior of color index B-V with phase angle in range of opposition effect.

The asteroid 1279 Uganda shows brightness behavior in range of opposition effect as E-type asteroids. But the spectrum in range of 0.45 – 0.99 mkm [3] is close to S-type with maximum on 0.77 mkm and extinction band centered near 0.9 mkm. It is necessary to perform the new observations of this asteroid for detail study of its magnitude- phase relation.

Conclusion: As a result of our program in this stage we carried out observations sixteen asteroids of different types and obtained magnitude- phase relations including low phase angles for ten asteroids. We detected very small opposition effect amplitude for dark asteroid 190 Ismene and beginning of OE at 1 deg for E- type asteroid 214 Aschera. We will plan to continue the program for study of brightness behavior at low phase angles and will carry out the new observations for distant objects.

References: [1] Belskaya I. N., and Shevchenko V. G. (2000) *Icarus 146*, 490-499. [2] Harris A. W., et al. (1989) *Icarus 81*, 365-374. [3] Xu S., et al. (1995) *Icarus 115*, 1-35. [4] Tholen D. .J. (1989) *In Asteroids II (Eds. Binzel, Gehrels, Matthews).* 1139-1150. [5] Bus S. J., Binzel R. P. (2002) *Icarus 158*, 146-177. [6] Lazzaro D., et al. (2004) *Icarus 172*, 179-220. [7] Tedesco E. F., et al. (2002) *Astron. J. 123*, 1056-1085.